

Surface topography modelling and ice flow velocity mapping of Dalk Glacier, East Antarctica: application of UAV remote sensing

Zheyi Cao^{1,2}, Leyue Tang^{1,2}, Xiaohan Yuan^{1,2}, Gang Qiao^{1,2*}

¹Center for Spatial Information Science and Sustainable Development Applications, Tongji University, Shanghai 200092, China

²College of Surveying and Geo-informatics, Tongji University, Shanghai 200092, China - 2133686@tongji.edu.cn, tly22@tongji.edu.cn, 1996yuanxiaohan@tongji.edu.cn, qiaogang@tongji.edu.cn

Keywords: remote sensing, surface topography modelling, ice flow velocity, unmanned aerial vehicle, Dalk Glacier, East Antarctica

Abstract

The Antarctic Ice Sheet is the largest potential contributor to global sea level rise due to global climate warming, making it important to monitor changes in the marginal outlet glacier dynamics and surface topography. The unmanned aerial vehicle (UAV), a new platform, has been proven to be a useful tool in glaciological applications because it can collect data in a variety of ways and has a high spatial and temporal resolution compared to traditional ground-based measurements and remote sensing from space. In this study, we used the combined UAV platform composed of the DJI Mavic 3 Enterprise (M3E) and M300 (L1) versions to perform high-accuracy on-site investigations of Dalk Glacier, a typical outlet glacier near the Zhongshan Station in East Antarctica. During the 39th Chinese Antarctic Expedition (CHINARE) in 2022-2023, UAV surveys with multiple sensors were performed. The M3E optical camera makes it possible to reconstruct high-resolution ortho-mosaic and digital elevation models (DEMs) of Dalk Glacier with high accuracy based on photogrammetric principles, helping us to extract the features of glacier surface topography, while dense point clouds derived from the L1 LiDAR camera are used to validate and improve the three-dimensional accuracy. To further monitor the dynamics and stability of Dalk Glacier, we generate ice flow velocity maps using ortho-mosaics for the years 2019, 2020, and 2023. The spatiotemporal changes in ice flow velocities were further compared with the products derived from satellite remote sensing data.

1. Introduction

The Antarctic Ice Sheet is the largest potential contributor to global sea level rise due to global climate warming, making it important to monitor changes in the marginal outlet glacier dynamics and surface topography (Depoorter et al., 2013).

Many outlet glaciers have undergone rapid changes in recent years. Calving events or reductions in ice-shelf thickness have been observed to significantly accelerate upstream tributary glaciation, leading to global mean sea level rise (Shepherd et al., 2010). Accelerated flow and ice thinning of huge ice shelves have been observed in West Antarctica, much of it in response to ocean forcing (Gudmundsson et al., 2019). Previous studies also show that changes in the dynamics of some outlet glaciers can lead to sea-ice conditions, subglacial floods, or intense melting (Fernando et al., 2015).

Remote sensing has become a powerful tool for glacier investigations. With large spatial coverage, satellite remote sensing cannot usually provide high-resolution details for glacier surface mapping (Bliakharskii et al., 2019). On the other hand, detailed in-situ surveys of Antarctic glaciers still have many limitations, including the cost of expeditions and unexpected weather conditions (Dering et al., 2019).

The unmanned aerial vehicle (UAV), a new platform, has been proven to be a useful tool in glaciological applications because it can collect data in a variety of ways and has a high spatial and temporal resolution compared to traditional ground-based measurements and remote sensing from space (Qiao et al., 2023). In recent years, with advantages in operation and safety, UAVs have been used in various aspects of polar research, such

as glacial geomorphology (Kreczmer et al., 2021), glacier topography (Benoit et al., 2019), and calving events (Chudley et al., 2019). It has been proven that more detailed analysis could be performed for glacier surface micro-topography studies in Antarctica based on UAV technology.

Dalk Glacier is a typical marine-terminating outlet glacier in East Antarctica. Previous studies of Dalk Glacier are fairly regular, making it one of the most studied glaciers in East Antarctica during the Chinese Antarctic Expedition (CHINARE). In this study, we aim to produce surface topography modelling and ice flow velocity mapping based on UAV observations.

2. Methods and Study Area

2.1 Study Area

Dalk Glacier (69°25'S, 76°27'E, Figure 1) is a typical marine-terminating outlet glacier on the Ingrid Christensen Coast of East Antarctica. It flows into the southeastern part of Prydz Bay east of Larsemann Hills, forming a floating ice shelf about 8 km long and 3 km wide (Chen et al., 2020).

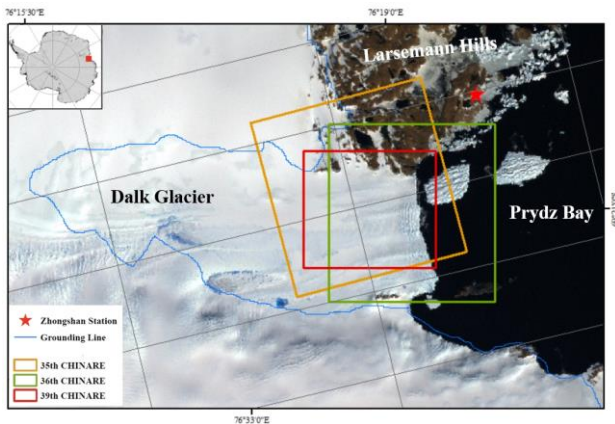


Figure 1. Location of the study area and UAV surveys on the background of the Landsat Image Mosaic of Antarctica (LIMA: <https://lima.usgs.gov/>).

2.2 UAV Platform for Photogrammetry

During the 39th CHINARE period from 2022 to 2023, we used the combined UAV platform composed of the DJI Mavic 3 Enterprise (M3E) and M300 (L1) (Figure 2) versions to perform high-accuracy on-site investigations. Meanwhile, D-RTK mobile stations are used to provide real-time differential data to M3E and M300 for centimeter-level geo-positioning.

The M3E optical camera makes it possible to reconstruct high-resolution ortho-mosaic and digital elevation models (DEMs) of the Dalk Glacier with high accuracy based on photogrammetric principles, helping us to extract the features of glacier surface topography, while dense point clouds derived from the M300 L1 LiDAR camera are used to validate and improve the three-dimensional accuracy.

Previous research (Yuan et al., 2020) has also proved that the combined UAV platform can achieve a relative mapping accuracy of centimetre-level, and the absolute position may have an offset of meter-level based on the positioning of the D-RTK mobile station.



Figure 2. Combined UAV platform composed of the DJI M3E and M300. (a) M3E. (b) M300. (c) D-RTK mobile station.

2.3 Image Processing

To model the surface topography of the Dalk Glacier, an automated integration of tie point measurements, camera calibration, DEM extraction, and true ortho-mosaic production has been implemented through Pix4Dmapper (<https://www.pix4d.com/product/pix4dmapper-photogrammetry-software>, Edition 4.4).

The structure-from-motion multi-view stereo technology (SfM-MVS) is employed to produce the orthophoto and three-dimensional surface model (Figure 3). After images covering the glacier surface were collected by the UAV platform, the internal and external parameters of the camera were then determined by using the camera calibration and direct geo-referencing techniques supported by the global navigation satellite system (GNSS) and inertial measurement unit (IMU) components. Then, feature detection and matching algorithms were applied to generate key points between images, while the camera position and orientation of each image were aligned and a sparse point cloud was generated by bundle adjustment. Based on the projection matrix derived from the camera parameters, the feature points in the images were mapped to the spatial coordinate system, and a dense point cloud was formed. Finally, the optimized point cloud was used to describe the characteristics of the regional space scene and to reconstruct the DEM and ortho-mosaic of the target area.

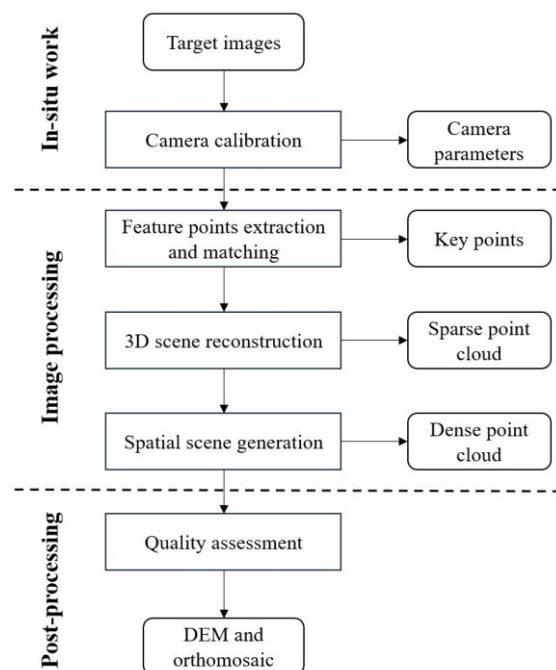


Figure 3. Main processes of SfM-MVS.

2.4 Template Matching for Ice Velocity

We used the Image Geo-Retification and Feature Tracking software (ImGRAFT: <http://imgraft.glaciology.net>) and the image matching techniques proposed by Li et al. (2017) to derive ice velocity fields for Dalk Glacier.

The hierarchical matching of feature points and grid points with additional triangulation constraints was further introduced to improve the accuracy and density of matching with a template window size of 32 pixels. Signal-to-noise thresholds, as well as the mean and standard deviation of the velocities, were employed to detect and eliminate noise.

2.5 Micro-topography of Dalk Glacier

Based on the ortho-mosaics, the surface micro-topography, such as ice melting, ice doline, and crevasses of the glacier terminus, can be observed in detail.

Besides, the ice front positions of Dalk Glacier were digitized based on both UAV data and Landsat-8 images from 2020 to 2023. The change in its terminus was quantified using the box method (Lea et al., 2014). The change in area between terminus observations of a fixed-width rectilinear box is converted to a 1-D value, representing the width-averaged terminus change, by dividing the area by the width of the box.

Uncertainty of the ice front position was caused by inaccuracy in manual digitization at about 0.5 pixels and the geolocation error of the image, which is estimated at 1 pixel based on the manually measured distance over stable features. Therefore, the total estimated error is around 1.5 pixels, which is acceptable in the range of similar studies (Miles et al., 2018).

3. Results

3.1 UAV Photogrammetry

During the 35th, 36th, and 39th CHINARE periods, three UAV survey missions (Figure 1) were performed near Larsemann Hills. All UAV surveys used vertical aerial photogrammetry for the micro-topography study. Before the implementation of each survey mission, a UAV remote controller was used to plan the flight route and set other flight parameters such as altitude and speed. We set the overlapping rate of the side and heading of the route at about 70-80% for better modelling accuracy. The flight route during the 39th CHINARE is displayed in Figure 4.

To further ensure an uninterrupted connection between D-RTK and the UAV and to avoid dangerous surface crevasses, the

UAV was launched and operated in the bare rock area of the Larsemann Hills near the western margin of the glacier with an open view. Each UAV survey was performed on a sunny day with low wind speeds.

Flight dates and other details of the UAV surveys are listed in Table 1.

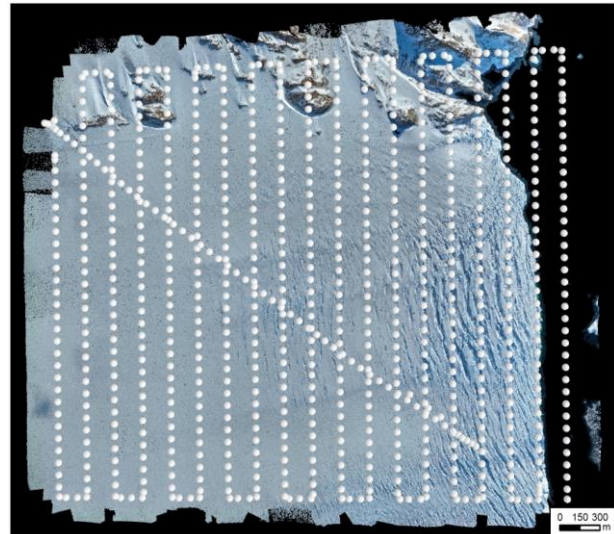


Figure 4. Camera location of each image displayed in Pix4Dmapper.

Date	Area (km ²)	Height (m)	Image number	Spatial resolution (m)	Horizontal accuracy (m)	Vertical accuracy (m)
2019/1/14 (35th CHINARE)	4.9	236	1,332	0.07	0.08	0.14
2020/1/3 (36th CHINARE)	10.7	356	1,221	0.11	0.14	0.20
2023/3/4 (39th CHINARE)	9.8	350	824	0.10	0.10	0.19

Table 1. Details and accuracy of three UAV surveys.

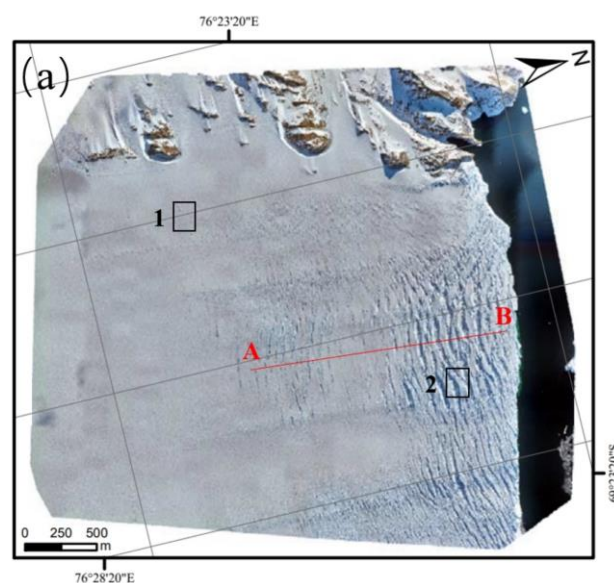
3.2 Terrain of Dalk Glacier

The surface topography of the Dalk Glacier was depicted by the high-resolution ortho-mosaic (Figure 5a) and DEM (Figure 5b) that were generated by the SfM-MVS method based on image data captured by the M3E camera, complemented by the LiDAR point cloud data collected by the M300 L1 camera.

In Figure 5a, the red line AB referred to the profile where the surface elevation changed significantly, and typical micro-topography was observed in Area 1 and Area 2 discussed in Section 3.4. The slope was then calculated based on DEM to further describe the topographic characteristics of the glacier surface (Figure 5c).

It could be observed that the elevation of the upstream regions of the Dalk Glacier changed slightly, and the slope was relatively small (Figure 5c). Upon reaching the terminus, the slope increased significantly, and a large number of crevasses appeared. In addition, in the central part of the leading edge of the ice shelf, a large ice rumple could be clearly visualized, with a particularly high level of ice crevasse development in the vicinity (Figure 5b). The elevation on the red profile (AB, Figure 5a) was shown in Figure 5d. Along the ice flow, the elevation gradually decreased from 110 m to 90 m. However, a rise of about 10 m in height and 200 m in length appeared at the

terminus of the glacier (Figure 5d), which might be correlated with the topography at the bottom of Dalk Glacier.



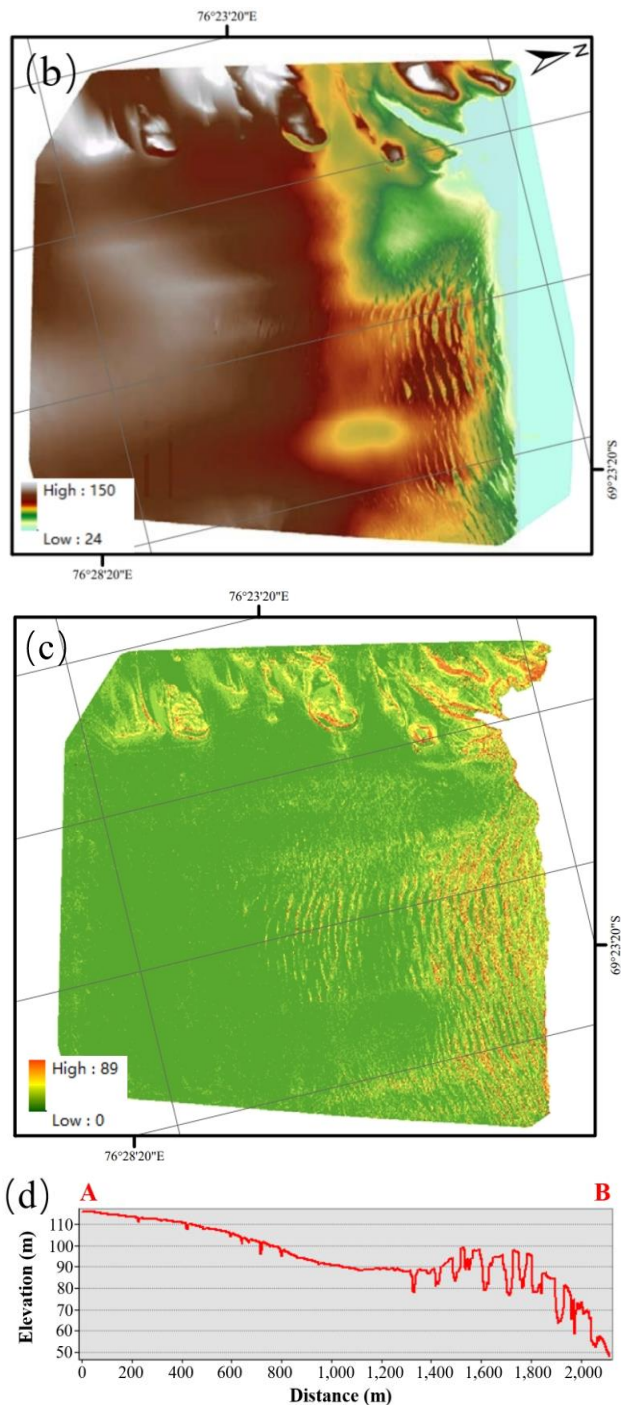


Figure 5. Modelling of Dalk Glacier during the 39th CHINARE period. (a) Ortho-mosaics. (b) DEM. (c) Slope. (d) Elevation profile of red line in (a).

3.3 Ice Velocity of Dalk Glacier

Two ice velocity maps were generated based on the co-registered ortho-mosaics of Dalk Glacier derived from UAV photogrammetry during the 35th, 36th, and 39th CHINARE campaigns, respectively, from 2018 to 2023 (Figure 1).

The accuracy was estimated by the bedrock area of Larsemann Hills where the ice velocity was close to zero, and the RMSE was calculated at about 3.81 m a^{-1} with a spatial resolution of 20 m. Figure 6b shows one of the ice velocity maps (240 m resolution) from the inter-mission time series of the land ice

velocity and elevation (ITS_LIVE) project. The error of the ITS_LIVE map was 20.01 m a^{-1} (Gardner et al., 2019), which showed that UAV-derived maps had advantages in terms of quality and spatial resolution.

The ice velocity map showed that the ice flow direction of Dalk Glacier was approximately south to north (Figure 6a). The ice velocity of the middle part of the glacier was much higher than that of upstream and marginal regions, and it eventually reached a maximum of about 290 m a^{-1} at its terminus area, which was larger than the maximum ice velocity of 240 m a^{-1} from the 2018 ITS_LIVE map (Figure 6b). According to the topographic characteristics of the glacier surface, the average ice velocity increase in the past three years might be related to numerous surface crevasses around the ice rumple. Previous studies suggested that the ice velocity increase after glacier calving might be related to the loss of buttressing provided by the ice rumple of the Dalk Glacier (Chen et al., 2020). However, more field and remote sensing observations with high resolution are needed to further understand the dynamics of Dalk Glacier.

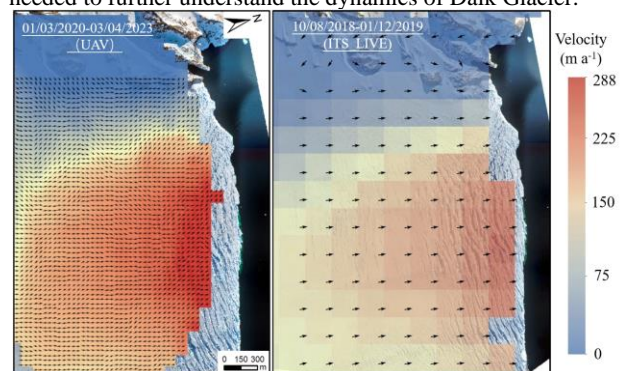


Figure 6. Ice velocity maps derived by UAV images (a) and from the ITS_LIVE project (b). The background is the UAV ortho-mosaic of Dalk Glacier.

3.4 Micro-topography of Dalk Glacier

In March 2023, it was not observed that melt-water and ice doline appeared on the surface of the glacier. However, a large area of snow bridges with few narrow crevasses (Figure 7a) was found near the Larsemann Hills corresponding to Area 1 in Figure 5a, which might threaten the safety of scientific research crews. A large number of crevasses (Figure 7b) appeared at the terminus of the Dalk Glacier referring to Area 2 in Figure 5a. The surface topography could reflect the outlet glacier dynamics system.



Figure 7. Micro-topography of Dalk Glacier terminus. (a) Snow bridges. (b) Crevasses.

Ice front positions were digitalized via UAV data and Landsat-8 images (Figure 8a). Overall, the terminus of Dalk Glacier has experienced cyclic change around the ice rumple in the last three years. In November 2020, Dalk Glacier had the largest ice front area; the ice front retreated by approximately 300 m between November 2020 and March 2021 (Figure 8b). From March 2021, the ice front continuously advanced at an average speed of about 100 m a⁻¹. Similar cyclic calving of the glacier terminus was also detected in 2006, 2009, 2011, and 2016 (Chen et al., 2020).

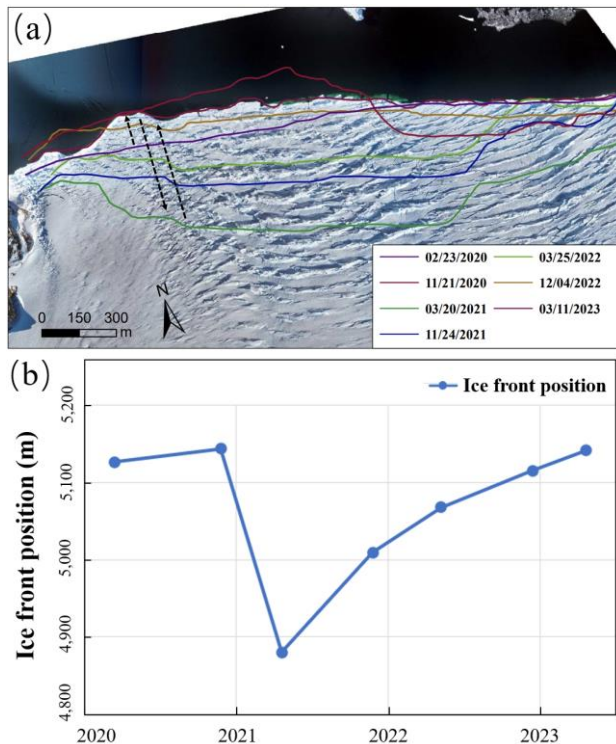


Figure 8. (a) Terminus position changes of Dalk Glacier from 2020 to 2023. The background is the UAV ortho-mosaic of the Dalk Glacier. (b) shows the quantified change of the ice front position of the glacier.

4. Conclusions and Future Work

In this study, high-resolution ortho-mosaic and digital elevation models of Dalk Glacier were reconstructed with high accuracy based on UAV photogrammetry. We also generated ice velocity using ortho-mosaics for the years 2019, 2020, and 2023. An unusual rise in terrain was observed in the middle of the Dalk Glacier terminus, accompanied by massive crevasses. Meanwhile, the micro-topography of glacier terrain and spatiotemporal changes in ice flow velocities were further analyzed which may reveal hints about the dynamics and stability of Dalk Glacier.

In future work, there are prospects for the application of UAVs in polar areas. UAV platforms with longer working endurance are necessary in extremely harsh environments. UAV platforms with various sensors are also needed to gain more important information for long-term investigation.

Acknowledgements

This work was supported by the National Key Research and Development Program of China (no. 2021YFB3900105, 2022YFC2807105), the National Natural Science Foundation of

China (grant no. 42276249, 42394131, and 42111530185), and Fundamental Research Funds for the Central Universities.

References

- Bhardwaj, A., Sam, L., Akanksha, Martín-Torres, F. J., & Kumar, R., 2016. UAVs as remote sensing platform in glaciology: present applications and future prospects. *Remote Sensing of Environment*, 175, 196-204. doi.org/10.1016/j.rse.2015.12.029
- Benoit, L., Gourdon, A., Vallat, R., Irarrazaval, I., Gravey, M., Lehmann, B., ... & Mariethoz, G., 2019. A high-resolution image time series of the gorner glacier-swiss alps-derived from repeated unmanned aerial vehicle surveys. *Earth System Science Data*, 11(2), 579-588. doi.org/10.5194/essd-11-579-2019.
- Bliakharskii, D. P., Florinsky, I. V., & Skrypitsyna, T. N., 2019. Modelling glacier topography in antarctica using unmanned aerial survey: assessment of opportunities. *International Journal of Remote Sensing*, 40(7), 2517-2541. doi.org/10.1080/01431161.2019.1584926.
- Chen, Y.; Zhou, C.; Ai, S.; Liang, Q.; Zheng, L.; Liu, R.; Lei, H., 2020. Dynamics of Dalk Glacier in East Antarctica Derived from Multisource Satellite Observations Since 2000. *Remote Sens.*, 12(11): 1809. doi.org/10.3390/rs12111809.
- Chudley, T. R., Christoffersen, P., Doyle, S. H., Abellan, A., & Snooke, N., 2019. High-accuracy uav photogrammetry of ice sheet dynamics with no ground control. *The Cryosphere*, 13(3), 955-968. doi.org/10.5194/tc-13-955-2019.
- Depoorter, M., Bamber, J., Griggs, J. et al., 2013. Calving fluxes and basal melt rates of Antarctic ice shelves. *Nature*, 502, 89–92. doi.org/10.1038/nature12567.
- Dering, G. M., Micklethwaite, S., Thiele, S. T., Vollgger, S. A., & Cruden, A. R., 2019. Review of drones, photogrammetry and emerging sensor technology for the study of dykes: Best practices and future potential. *Journal of Volcanology and Geothermal Research*, 373, 148–166. doi.org/10.1016/j.jvolgeores.2019.01.018.
- E. Rignot et al., 2013. Ice-Shelf Melting Around Antarctica. *Science*, 341, 266-270. https://doi.org/10.1126/science.1235798.
- Fernando, S., 2015. Volume loss from Antarctic ice shelves is accelerating. *Science*, 348, 327-331. https://doi.org/10.1126/science.aaa0940.
- Florinsky, I. V., & Bliakharskii, D. P., 2019a. Detection of crevasses by geomorphometric treatment of data from unmanned aerial surveys. *Remote sensing letters*, 10(4), 323-332. doi.org/10.1080/2150704X.2018.1552809.
- Gardner, A. S., Fahnestock, M. A., & Scambos, T. A., 2019. MEaSUREs ITS_LIVE Landsat image-pair glacier and ice sheet surface velocities. *Version*, 1. doi.org/10.5067/IMR9D3PEI28U.
- Gudmundsson, G. H., Paolo, F. S., Adusumilli, S., & Fricker, H. A., 2019. Instantaneous Antarctic ice-sheet mass loss driven by thinning ice shelves. *Geophysical Research Letters*, 46, 13903–13909. doi.org/10.1029/2019GL085027.
- Immerzeel, W. W., Kraaijenbrink, P. D. A., Shea, J. M., Shrestha, A. B., Pellicciotti, F., Bierkens, M. F. P., & De Jong, S. M., 2014. High-resolution monitoring of Himalayan glacier dynamics u

- sing unmanned aerial vehicles. *Remote Sensing Environment*, 150, 93–103. doi.org/10.1016/j.rse.2014.04.025.
- Jouvet, G., Weidmann, Y., Kneib, M., Detert, M., Seguinot, J., Sakakibara, D., & Sugiyama, S., 2018. Short-lived ice speed-up and plume water flow captured by a vtol uav give insights into subglacial hydrological system of Bowdoin Glacier. *Remote Sensing of Environment*, 217, 389-399. doi.org/10.1016/j.rse.2018.08.027
- Kreczmer, K., Dąbski, M., Zmarz, A., 2021. Terrestrial Signature of a Recently-Tidewater Glacier and Adjacent Periglaciation, Windy Glacier (South Shetland Islands, Antarctic). *Front. Earth Sci.*, 9, 671985. doi.org/10.3389/feart.2021.671985.
- Kristaps, L., Janis, K., Maris, K., Jurijs, J., 2020. High-resolution orthophoto map and digital surface models of the largest Argentine Islands (the Antarctic) from unmanned aerial vehicle photogrammetry. *Journal of Maps*, 16:2, 335-347. doi.org/10.1080/17445647.2020.1748130.
- Lea, J.M., Mair, D.W.F., Rea, B.R., 2014. Evaluation of existing and new methods of tracking glacier terminus change. *J. Glaciol.*, 60, 323–332. doi.org/10.3189/2014JoG13J061.
- Li, R., Ma, X., Cheng, Y., Ye, W., Guo, S., Tang, G., Wang, Z., Gao, T., Huang, Y., Li, X., Qiao, G., Tian, Y., Feng, T., Tong, X., 2017. Ice Velocity Measurement in East Antarctica from 1960s to 1980s based on Argon and Landsat Imagery. *The International Archives of the Photogrammetry, Remote Sensing and Spatial Information Sciences*, XLII-2/W7, 1535–1539. doi.org/10.5194/isprs-archives-XLII-2-W7-1535-2017.
- Li, R., Ye, W., Qiao, G., Tong, X., Liu, S., Kong, F., Ma, X., 2017. A New Analytical Method for Estimating Antarctic Ice Flow in the 1960s From Historical Optical Satellite Imagery. *IEEE Transactions on Geoscience and Remote Sensing*, 55, 2771–2785. doi.org/10.1109/TGRS.2017.2654484.
- Li, Y., Qiao, G., Popov, S., Cui, X., Florinsky, I., Yuan, X., & Wang, L., 2023. Unmanned aerial vehicle remote sensing for Antarctic research. *IEEE Geoscience and Remote Sensing Magazine*, 11(1), 73-93. doi.org/10.1109/MGRS.2022.3227056.
- Miles, B.W.J., Stokes, C.R., Jamieson, S.S.R., 2018. Velocity increases at Cook Glacier, East Antarctica, linked to ice shelf loss and a subglacial flood event. *The Cryosphere*, 12, 3123–3136. doi.org/10.5194/tc-12-3123-2018.
- Qiao, G., Yuan, X., Florinsky, I., Popov, S., He, Y., Li, H., 2023. Topography reconstruction and evolution analysis of outlet glacier using data from unmanned aerial vehicles in Antarctica. *International Journal of Applied Earth Observation and Geoinformation*, 117. doi.org/10.1016/j.jag.2023.103186.
- Ryan, J. C., Hubbard, A. L., Box, J. E., Todd, J., Christoffersen, P., Carr, J. R., Holt, T. O., & Snooke, N., 2015. UAV photogrammetry and structure from motion to assess calving dynamics at Store glacier, a large outlet draining the Greenland ice sheet. *Cryosphere*, 9(1), 1–11. doi.org/10.5194/tc-9-1-2015.
- Shepherd, A., Wingham, D., Wallis, D., Giles, K., Laxon, S., and Sundal, A. V., 2010. Recent loss of floating ice and the consequent sea level contribution, *Geophys. Res. Lett.*, 37, L13503. https://doi.org/10.1029/2010GL042496.
- Yuan, X., Qiao, G., Li, Y., Li, H., Xu, R., 2020. Modelling of glacier and ice sheet micro-topography based on unmanned aerial vehicle data, Antarctica. *Int. Arch. Photogramm. Remote Sens. Spat. Inf. Sci.* XLIII-B3-2020, 919–923. doi.org/10.5194/isprs-archives-XLIII-B3-2020-919-2020.
- Yao, H., Qin, R., & Chen, X., 2019. Unmanned aerial vehicle for remote sensing applications - a review. *Remote Sensing*, 11(12). doi.org/10.3390/rs11121443